Intracellular Viral Life-cycle Induced Rich Dynamics in Tumor Virotherapy

Jianjun Paul Tian[1], Yang Kuang[2], Hanchun Yang[3]
[1]Department of Mathematics
The College of William and Mary, Williamsburg, VA 23187
[2] School of Mathematical and Statistical Sciences
Arizona State University, P.O. Box 871804 Tempe, AZ 85287
[3] Department of Mathematics
Yunnan University, Kunming 650091, PR China

Emails: jptian@math.wm.edu, kuang@asu.edu, hyang@ynu.edu.cn

Abstract

The intracellular viral life-cycle is an important process in tumor virotherapy. Most mathematical models for tumor virotherapy do not incorporate the intracellular viral life-cycle. In this article, a model for tumor virotherapy with the intracellular viral life-cycle is presented and studied. The period of the intracellular viral life-cycle is modeled as a delay parameter. The model is a nonlinear system of delay differential equations. It displays interesting and rich dynamic behaviors. There exists two sets of stability switches as the period of the intracellular viral life-cycle increases. One is around the infection free equilibrium solution, and the other is the positive equilibrium solution. This intracellular viral life-cycle may explain the oscillation phenomena observed in many studies. An important clinic implication is that the period of the intracellular viral life-cycle should also be modified when a type of a virus is modified for virotherapy, so that the period of the intracellular viral life-cycle is in a suitable range which can break away the stability of the interior equilibrium solution.

1 Introduction

The old hypothesis of viruses can be used to kill tumor cells has been extensively restudied over last 20 years. Oncolytic viruses have been identified in many experiences [3]. Viruses that can infect and replicate in cancer cells but leave healthy cells unharmed can serve as oncolytic viruses. In an ideal situation, when oncolytic viruses are inoculated into a cancer patient or directly injected into a tumor, they spread throughout the tumor, and infect tumor cells. The viruses that enter into tumor cells will replicate themselves. Upon a lysis of an infected tumor cell, a swarm of new viruses burst out and infect neighboring tumor cells. It was hypothesized that all tumor cells would be infected and the tumor would be eradicated since the beginning of the nineteenth century [8]. However, most often the viral infection was stopped by the host immune system and failed to impact on tumor growth. The later technology of reverse genetics has brought about new methods to generate tumor-selective viruses, and progresses in understanding of the molecular mechanism of viral cytotoxicity of oncolytic viruses may provide a fascinating therapeutic approach to cancer patients. Recent experiments in animal brain tumors using genetically engineered viral strains, such as adenovirus, ONYX-15 and CV706, herpes simplex virus 1 and wild-type Newcastle disease virus show these viruses to be relatively non-toxic and tumor specific [9]. However, the therapeutic effects of these oncolytic viruses are not well established yet.

There are many factors that influence the efficacy of tumor virotherapy. The major factors include the intracellular viral life-cycle and viral replication within tumor cells, viral localization or virus distribution within a tumor, and the immune responses that viral infection induce [12]. Many experiments with animals and phase I clinical trials have been conducted to investigate these factors. For example, a great deal of the intracellular viral life cycle has been found out experimentally. In [3], the intracellular viral life cycle for adenovirus and herpes simplex virus (HSV)-1 is detailed, "the life cycle can be divided into several stages. During the infection stage,

viral surface proteins, such as the adenovirus fibre or HSV glycoprotein D, mediate attachment to cellular receptors, such as coxsackie and adenovirus receptor (CAR) or HSV entry mediator C (HVEC), also known as nectin 1. Once inside the cell, viruses express several gene products that target cellular proteins and modulate various cellular processes, such as preventing apoptosis or inducing cell-cycle entry. These promote viral replication and production of viral proteins that eventually lead to cell lysis and release of viral progeny". Each step is mediated by a diverse group of proteins, and each step needs some time to complete [6, 7, 4, 13]. However, an integrated and quantitative understanding of viral kinetics is required in order to find predictive factors for the efficacy of virotherapy. Without such an understanding, much of the clinical research will continue to be based on trial and error. In this aspect, mathematical modeling can allow us to see the whole spectrum of possible outcomes, and provide the rationale to optimize treatments. Several attempts have been made to understand and characterize viral dynamics by mathematical models [5, 14, 16, 15, 17, 18, 19, 1, 20]. These studies are largely of qualitative simulation in nature and examine how variation in viral and host parameters influences the outcomes of treatments. The outcomes of virotherapy depend in a complex way on interactions between viruses and tumor cells. A clearer picture of the dynamics of virotherapy needs to be developed.

Based on experimental results in [10] that glioma-selective HSV-1 mutants (rQNestin34.5) have a high replication ability and doubles the life span of glioma mice. The studies in [5, 14] have suggested that viral replication ability is one of major factors for the success of virotherapy. The model in [5] studies interactions among glioma cells, infected glioma cells, viruses, immune cells, and also includes the immunosuppressive agent, cyclophosphamide. It is a nonlinear parabolic system with a free boundary as tumor surface. The study of a space-free virotherapy model in [14] suggests that the oscillation is an intrinsic property of virotherapy dynamics and relates to virus replication ability. The present paper focuses on analyzing the effect of the intracellular viral life-cycle on the dynamics of oncolysis in a relatively

simpler setting and will only consider tumor cells and viruses in a space-free setting.

The rest of the article is organized as follows. In Section 2, the mathematical model is introduced. In Section 3, preliminary results on the model are presented. In Section 4, the stability of the equilibrium solutions is studied, and some numerical analysis is also presented. In Section 5, we conclude the paper by a discussion of biological implications of our results.

2 Mathematical models

Wodarz and Komarova in [11, 18, 19] proposed the following general model of tumor cell and infected tumor cell growth based on the mass action law,

$$\begin{aligned} x' &= \frac{dx}{dt} = xF(x,y) - \beta y G(x,y), \\ y' &= \frac{dy}{dt} = \beta y G(x,y) - ay, \end{aligned} \tag{1}$$

where x stands for the uninfected tumor cell population and y the infected tumor cell population. The function F describes the growth properties of the uninfected tumor cells with $F(0,0)$ representing their maximum growth rate, and the function G describes the rate at which tumor cells become infected by the virus. These two functions may take various forms, depending on how much detail of the biology is incorporated into the model. The coefficient β represents the strength of infectivity of the virus via infected tumor cells. The infected tumor cells die at a rate ay. We would like to point out that this is a reduced basic framework to describe the dynamics of virotherapy. Generally, infected tumor cells can not infect uninfected tumor cells directly; only free viruses that are in extracellular matrix can infect tumor cells. For this reason, the above model shall be understood as an approximation of

the following model with explicit virus dynamics

$$\begin{aligned} x' &= \frac{dx}{dt} = xF(x,y) - bvg(x,y), \\ y' &= \frac{dy}{dt} = bvg(x,y) - ay, \\ v' &= \frac{dy}{dt} = ky - dv, \end{aligned} \tag{2}$$

where $\min\{k,d\} >> F(0,0)$, and $\beta yG(x,y) = \frac{bk}{d} yg(x,y)$. Here $vg(x,y)$ describes the contact rate of virus with uninfected tumor cells, b is the virus infection coefficient (rate), k stands for the virus production rate of an infected cell and d is the death rate of virus. In other words, one may take advantage of the fact that virus dynamics is usually much faster than that of tumor cell by approximating v with $\frac{k}{d}y$ in the above model.

There are several stages in a typical viral life-cycle. The first stage is the attachment stage. When a free virus is within a certain distance of a tumor cell, chemical bonds form between the virus and receptor sites of the tumor cell, and then attach to tumor cell surface. The second is the penetration stage, where the viral DNA passes through the core and into the tumor cell. Once the virus penetrates into the tumor cell, the biosynthesis stage begins. Since the virus expresses several gene products that target cellular proteins and modulate various cellular processes, the host protein synthesis stop and the host transcription and translation are interfered. Meantime, the virus uses host nucleotides to replicate its DNA and use host ribosomes, enzymes and amino acids to synthesize its enzymes and proteins. During the maturation stage, viral capsids are assembled, viral DNA are packed into the heads and tails fibers are joined to the complexes. The last step is the release stage. The newly-born viruses are released from the tumor cell, and the tumor cell dies. The time period of the intracellular viral life-cycle varies according to virus species, it changes from minutes to days. For the details of the viral life-cycle, we refer the reader to [3, 6, 7, 4, 13] While it may not be necessary to include all details of the viral life-cycle into a mathematical model where we are mainly interested in tumor dynamics to void complication, it is interesting to find out what dynamics maybe induced

by the intracellular viral life-cycle in a tumor virotherapy. A simple way to study the intracellular viral life-cycle induced dynamics is to incorporate a cycle time delay parameter in a plausible model.

Let the cycle time of the intracellular viral life-cycle be τ, defined to be the period of time from a virus attaching to a tumor cell to new viruses bursting out. We assume a constant death rate for infected but not yet virus-producing tumor cells to be n. Then the probability of infected tumor cells surviving the time period from $t-\tau$ to t is $e^{-n\tau}$. (More generally, the survival probability is given by some nonincreasing function $p(\tau)$ between 0 and 1.) For simplicity, we lump the natural death of infected tumor cells and death by bursting together. This yields

$$\begin{aligned}\frac{dx}{dt} &= xF(x,y) - \beta y G(x,y),\\ \frac{dy}{dt} &= \beta y(t-\tau)G(x(t-\tau),y(t-\tau))e^{-n\tau} - ay.\end{aligned}$$

In the following, we take $F(x,y) = r(1-\frac{x+y}{K})$ and $G(x,y) = x$, where r is per capital growth rate of the tumor, and K is the maximum of the tumor cell load. Therefore, the model we will focus on is given by,

$$\begin{aligned}\frac{dx}{dt} &= rx(1-\frac{x+y}{K}) - \beta xy,\\ \frac{dy}{dt} &= \beta x(t-\tau)y(t-\tau)e^{-n\tau} - ay,\\ x(\theta) &\geq 0, y(\theta) \geq 0, \text{are continuous on } [-\tau, 0),\\ x(0) &> 0, y(0) > 0.\end{aligned} \tag{3}$$

3 Preliminaries

For the convenience of analysis, we non-dimensionalize the system by setting $\bar{x} = \frac{x}{K}$, $\bar{y} = \frac{y}{K}$, and then drop the bar over the variables. We get the non-dimensionalized system,

$$\begin{aligned}
\frac{dx}{dt} &= rx(1-x-y) - bxy, \\
\frac{dy}{dt} &= bx(t-\tau)y(t-\tau)e^{-n\tau} - ay, \\
x(\theta) \geq 0, y(\theta) \geq 0, &\quad x(\theta), y(\theta) \in C[-\tau, 0],
\end{aligned} \tag{4}$$

where $b = \beta K$. We remark that all parameters here are nonnegative.

As an epidemiology model at the cell population level, the basic reproduction number is given by

$$R_0 = \frac{\beta}{a} e^{-n\tau} = \frac{b}{aK} e^{-n\tau}.$$

However, we will not use this quantity as a critical value to characterize the dynamics of the model (4), since there is the parameter τ presenting the period of the intracellular viral life-cycle, and we are more interested in how this parameter affects the dynamics.

We will study the feasible region and positivity of the solutions of this system, and the existence of equilibrium solutions.

Proposition 3.1. *Let $0 \leq x(\theta), y(\theta) \leq 1$ for $\theta \in [-\tau, 0)$, and $x(0) > 0$, $y(0) > 0$. Then the solution of the system (4) $x(t) > 0$, $y(t) > 0$, and $x(t) < 1$. When $x(0) + y(0) < 1$, we have $x(t) + y(t) < 1 + \frac{b}{r} e^{-n\tau}$ for $t \geq 0$.*

Proof. When $0 \leq t \leq \tau$, we see that $y' = bx(t-\tau)y(t-\tau)e^{-n\tau} - ay \geq -ay$, so $y(t) > y(0)e^{-at} > 0$. In addition, $x' = rx(1-x-y) - bxy$, so $x(t) = x(0)e^{\int_0^t r(1-x(s)-y(s)-\frac{b}{r}y(s))ds} > 0$. By the method of steps, $x(t) > 0$ and $y(t) > 0$ for all $t > 0$.

For $x' = rx(1-x-y) - bxy < rx(1-x)$, so, $x(t) < 1$.

For $0 \leq t \leq \tau$, adding the two equations of the system (4) together, we have $x' + y' = rx(1-x-y) - bxy + be^{-n\tau}x(t-\tau)y(t-\tau) - ay \leq rx(1-x-y) - bxy + be^{-n\tau} - ay \leq rx(1-x-y) + be^{-n\tau} \leq r(1 + \frac{b}{r}e^{-n\tau} - x - y)$. When $x(0) + y(0) < 1$, by a standard comparison argument, we have $x(t) + y(t) < 1 + \frac{b}{r}e^{-n\tau}$. By the method of steps, the estimate holds for $t \geq 0$. □

Therefore, We will consider our system over this region, and the global word will refer to this region.

The system always has equilibria $(0,0)$ and $(1,0)$ for any values of parameters. The interior equilibrium solution (x^*, y^*) is given by

$$E^* = (x^*(\tau), y^*(\tau)) = (\frac{a}{b}e^{n\tau}, \quad \frac{1-\frac{a}{b}e^{n\tau}}{1+\frac{b}{r}}).$$

It should be noticed that the interior equilibrium is a function of the model parameters, and we will mainly consider it as a function of delay parameter τ.

Since the time delay parameter τ can not be negative in our case, when $b \leq a$, there are only two nonnegative equilibria, $(0,0)$ and $(1,0)$. When $b > a$, there are two cases. If $0 < \tau < \frac{1}{n}\ln\frac{b}{a}$, there are three nonnegative equilibria. At $\tau = \frac{1}{n}\ln\frac{b}{a}$, the interior equilibrium (x^*, y^*) merges to $(1,0)$. If $\tau > \frac{1}{n}\ln\frac{b}{a}$, the interior equilibrium has negative components and goes out of the feasible region. We will not consider this case. So, when $\tau \geq \frac{1}{n}\ln\frac{b}{a}$, there are only two nonnegative equilibria, $(0,0)$ and $(1,0)$.

The Figure 1 shows the planar analysis of isoclines and the interior equilibrium curve as the delay parameter τ. It also makes clear how the interior equilibrium point $(x^*(\tau), y^*(\tau))$ depends on the delay τ and other parameters. For instant, increasing τ moves the y-isoline towards right, and causes the coincidence of $(x^*(\tau), y^*(\tau))$ with $(1,0)$ at a finite value of τ. For large τ there is no positive interior equilibrium point. We will track how the interior equilibrium depends on the parameters in all our analysis.

4 Analysis of the model

In this section, the local stability analysis of the three equilibria and some global stability analysis will be conducted. The stability switches around the equilibria $(1,0)$ and $(x^*(\tau), y^*(\tau))$ will also be studied.

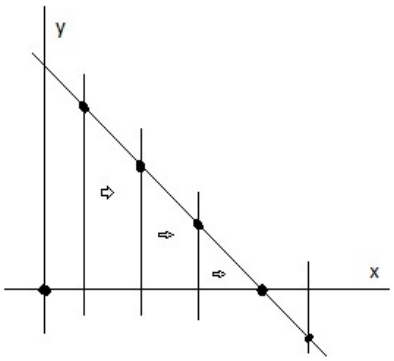

Figure 1: For various values of the delay parameter τ, the isoclines of the system are obtained from (4) by removing the delay parameters from the argument. The arrows indicate the y-isoclines change as τ increases, while the dots indicate equilibria.

4.1 Stability of the equilibrium $(0, 0)$

At the equilibrium point $(0, 0)$, the linearization is

$$\frac{dx}{dt} = rx,$$
$$\frac{dy}{dt} = -ay.$$

The eigenvalues are r and $-a$. It is a saddle point. The stable manifold is in $y-$aixs, and the unstable manifold is in $x-$axis. This means that the tumor will grow when it starts with a very small size, while the tumor with only infected cells will shrink to zero.

4.2 Stability of the equilibrium $(1, 0)$

At the equilibrium point $(1, 0)$, we linearize the system by setting $x = 1 + \bar{x}$ and $y = \bar{y}$, we have

$$\begin{aligned}\bar{x}' &= -r\bar{x} - r\bar{y} - r\bar{x}^2 - r\bar{x}\bar{y} - b\bar{y} + \cdots,\\ \bar{y}' &= -ay + b\bar{y}(t-\tau)e^{-n\tau} + b\bar{x}(t-\tau)\bar{y}(t-\tau)e^{-n\tau}.\end{aligned}$$

The linear system then is given by

$$\begin{pmatrix} \bar{x}' \\ \bar{y}' \end{pmatrix} = \begin{pmatrix} -r & -r-b \\ 0 & -a \end{pmatrix} \begin{pmatrix} \bar{x} \\ \bar{y} \end{pmatrix} + \begin{pmatrix} 0 & 0 \\ 0 & be^{-n\tau} \end{pmatrix} \begin{pmatrix} \bar{x}(t-\tau) \\ \bar{y}(t-\tau) \end{pmatrix}. \quad (5)$$

The characteristic equation is $|\lambda I - A - Be^{-\lambda\tau}| = 0$, where the matrices A and B are given in (5). Or, $(\lambda + r)(\lambda + a - be^{-n\tau}e^{-\lambda\tau}) = 0$. So, one eigenvalue is $-r$, the other eigenvalues are given by

$$\lambda + a - be^{-n\tau}e^{-\lambda\tau} = 0. \quad (6)$$

We study the roots of the equation (6) according to the relation between a and b. Denote the root by $\lambda(\tau) = \alpha(\tau) + i\omega(\tau)$.

When $b < a$, $\lambda(0) = b - a < 0$. Suppose $\lambda = i\omega$ is a root of (6), where $\omega > 0$. Then, substitute it into (6), we have $i\omega + a - be^{-n\tau}e^{-i\omega\tau} = 0$. Separate the real parts and imaginary parts. One has, $\omega + be^{-n\tau}\sin\omega\tau = 0$ and $a - be^{-n\tau}\cos\omega\tau = 0$. By $\sin^2\omega\tau + \cos^2\omega\tau = 1$, one gets $b^2e^{-2n\tau} = \omega^2 + a^2$. Then, $\omega^2 = b^2e^{-2n\tau} - a^2 < 0$. This is impossible. Therefore, the sign of the real part of the root $\lambda(\tau)$ keeps unchangeable for all $\tau \geq 0$. Namely, $\alpha(\tau) < 0$ for any $\tau \geq 0$. In this case, the equilibrium point $(1, 0)$ is locally asymptotical stable for any (zero or positive) delay. Consequently, there is no stability switches around the equilibrium point $(1, 0)$ when $b < a$. For the details about stability switching, we refer the paper [2] by Beretta and Kuang.

If $a = b$, we claim that the real part of any root of the characteristic equation (6) is negative. Suppose $\lambda = u + iv$, then substitute it into the equation. Separate the real part and imaginary part, we have $u + a -$

$ae^{-(n+u)\tau}\cos v\tau = 0$ and $v + ae^{-(n+u)\tau}\sin v\tau = 0$. Square them and add them together, we have $(u+a)^2 + v^2 = a^2e^{-2(n+u)\tau}$. For any $\tau > 0$ and positive parameter n, if $u > 0$, then $(u+a)^2 + v^2 > a^2$ and $a^2e^{-2(n+u)\tau} < a^2$. This is a contradiction. If $u = 0$, we arrive the same contradiction. Therefore, when $a = b$, the equilibrium $(1, 0)$ is still asymptotically stable for any positive delay $\tau > 0$.

When $b > a$, $\lambda(0) = \alpha(0) + i\omega(0) = b - a > 0$. Then, there is a positive eigenvalue at $\tau = 0$. We search for the values of the delay τ at which the sign of the real part of $\lambda(\tau)$ changes, where we have stability switches. Suppose $\lambda = i\omega$ is a root, $\omega > 0$. One again obtains $i\omega + a - be^{-n\tau}e^{-i\omega\tau} = 0$. Separate the real part and imaginary part, we have $\omega + be^{-n\tau}\sin\omega\tau = 0$ and $a - be^{-n\tau}\cos\omega\tau = 0$, and $\omega^2 = b^2e^{-2n\tau} - a^2$. Then

$$\omega(\tau) = (b^2e^{-2n\tau} - a^2)^{\frac{1}{2}},$$

where $\tau < \tau_c = \frac{1}{n}\ln\frac{b}{a}$. When $\tau > \tau_c$, there is no stability switches. As the method in [2], we define the angle $\theta(\tau) \in [0, 2\pi]$ which are the solutions of the equations for the real part and imaginary part as follows,

$$\sin\theta(\tau) = -\frac{\omega(\tau)}{b}e^{n\tau}, \quad \cos\theta(\tau) = \frac{a}{b}e^{n\tau}.$$

It is easy to see that $\theta(\tau)$ is in between $\frac{3}{2}\pi$ and 2π since a, b, and ω are positive. So, $\theta(\tau) = 2\pi - \arcsin\frac{\omega(\tau)}{b}e^{n\tau}$. We define

$$\tau_m(\tau) = \frac{\theta(\tau) + 2m\pi}{\omega(\tau)} = \frac{2(m+1)\pi - \arcsin\frac{\sqrt{b^2e^{-2n\tau} - a^2}e^{n\tau}}{b}}{\sqrt{b^2e^{-2n\tau} - a^2}}$$

for $m \in N_0$. The occurrence of stability switches may take place at the zeros of the functions

$$S_m := \tau - \tau_m(\tau), \quad m \in N_0. \tag{7}$$

To determine how many zeros of the functions (7) can have, we study the function

$$Z_m(\tau) = \tau\sqrt{b^2e^{-2n\tau} - a^2} + \arcsin\frac{e^{n\tau}}{b}\sqrt{b^2e^{-2n\tau} - a^2} - 2(m+1)\pi. \tag{8}$$

The function (8) has the same zeros as the function (7). The derivative of the function (8) is given by

$$Z'_m = \frac{b^2(1-n\tau)e^{-2n\tau} - a^2(n+1)}{\sqrt{b^2e^{-2n\tau} - a^2}}. \tag{9}$$

The critical points of Z_m, namely zeros of Z'_m are the same as its numerator, $b^2(1-n\tau)e^{-2n\tau} - a^2(n+1) = 0$. Then we have $(2-2n\tau) = \frac{2a^2(n+1)}{b^2}e^{2n\tau}$. By simply plotting functions $y = 2-x$ and $y = Ae^x$, it is easy to conclude that there is only one positive critical point for Z_m when $\frac{a^2(n+1)}{b^2} < 1$, there is only one zero critical point when $\frac{a^2(n+1)}{b^2} = 1$, and there is only one negative critical point when $\frac{a^2(n+1)}{b^2} > 1$. Since there is only one critical point, it easy to check at the critical point the function Z_m reaches its global maximum. Denote the critical point by τ_c, we arrive the conclusion that there will be two positive zeros for the function S_m when $\frac{a^2(n+1)}{b^2} < 1$ and $Z_m(\tau_c) > 0$ for some m. Although there would be one positive zero for S_m when $\frac{a^2(n+1)}{b^2} \geq 1$ and $Z_m(0) > 0$ for some m, we know the number of zeros of S_m only can be an even number.

To determine the ranges of parameter values where the pair of simple conjugate purely imaginary roots crosses the imaginary axis from left to right or from right to left, we use the theorems 3.1 and 3.2 in [2] to determine the sign of the derivative of the eigenvalue with respective to τ, $R(\tau) = sign\{\frac{dRe\lambda}{d\tau}\mid_{\lambda=i\omega(\tau^*)}\}$, and

$$\begin{aligned} R(\tau) =& sign\ \{a^2(\tau)\omega(\tau)\omega'(\tau)(a(\tau)b(\tau) + c(\tau)^2\tau) \\ &+ \omega^2(\tau)a^2(\tau)(a'(\tau)b(\tau) - a(\tau)b'(\tau) + c^2(\tau))\}, \end{aligned}$$

where $a(\tau) = 1$, $b(\tau) = a$ and $c(\tau) = -be^{-n\tau}$ for the characteristic equation (6). Then we have

$$\begin{aligned} R(\tau) &= sign\ \{\omega\omega'(a + b^2e^{-2n\tau}\tau) + \omega^2b^2e^{-2n\tau}\} \\ &= sign\ \{b^2e^{-2n\tau}(-na - a^2 - nb^2\tau e^{-2n\tau} + b^2e^{-2n\tau})\} \\ &= sign\ \{b^2e^{-2n\tau}[-a(a+n) + (1-n\tau)b^2e^{-2n\tau}]\} \end{aligned}$$

Therefore, $R(\tau) = +1$ if and only if $(1-n\tau)e^{-2n\tau} > \frac{a(a+n)}{b^2}$, and $R(\tau) = -1$ if and only if $(1-n\tau)e^{-2n\tau} < \frac{a(a+n)}{b^2}$.

We summarize what we get above as a theorem.

Theorem 4.1. *When $b < a$, the equilibrium $(1, 0)$ is locally asymptotically stable for $\tau \geq 0$. When $b \leq a$, the equilibrium $(1, 0)$ is locally asymptotically stable for $\tau > 0$. When $b > a$, $b^2 > a^2(1 + n)$, and $Z_m(\tau_c) > 0$, there are two values, $\tau_1 < \tau_2$, of the delays, at which the stability switches occur. Moreover, $R(\tau_1) = -1$ if $(1 - n\tau)e^{-2n\tau} < \frac{a(a+n)}{b^2}$, and $R(\tau_2) = +1$ if $(1 - n\tau)e^{-2n\tau} < \frac{a(a+n)}{b^2}$, the equilibrium $(1, 0)$ is unstable when $0 \leq \tau < \tau_1$ or $\tau > \tau_2$, it is locally asymptotically stable when $\tau_1 < \tau < \tau_2$.*

In fact, the equilibrium solution $(1, 0)$ is globally stable when $b < a$ or $b \leq a$.

Theorem 4.2. *When $b \leq a$, the equilibrium solution $(1, 0)$ is globally stable on the region Δ for any positive time delay $\tau > 0$. When $b < a$, the equilibrium $(1, 0)$ is globally stable on the region Δ for any nonnegative time delay $\tau \geq 0$.*

Proof. From the proposition (3.1), $y(t) \geq 0$ and $0 \leq x(t) \leq 1$, we have $\liminf_{t\to\infty} y(t) \geq 0$ and $\limsup_{t\to\infty} x(t) \leq 1$.

To estimate $y(t)$, we have $y' = bx(t - \tau)y(t - \tau)e^{-n\tau} - ay \leq be^{-n\tau}y(t - \tau) - ay$. To use comparison theorem, we look at the equation $\dot{u} = be^{-n\tau}u(t - \tau) - au$. Since $be^{-n\tau} < b \leq a$ for $\tau > 0$ or $be^{-n\tau} \leq b < a$ for $\tau \geq 0$, then $\lim_{t\to\infty} u(t) = 0$. Thus, $y(t) \leq u(t)$, and $\limsup_{t\to\infty} y(t) \leq 0$. Therefore, $\lim_{t\to\infty} y(t) = 0$.

For any ε, there is $T > \tau$, such that $y(t) < \varepsilon$ when $t > T$. Then, we have $x' = rx(1-x-y)-bxy \geq rx(1-x-\varepsilon)-b\varepsilon x = rx(1-\varepsilon-b\varepsilon-x)$. By a standard comparison argument, $x(t) \geq 1 - \varepsilon - b\varepsilon$, and $\liminf_{t\to\infty} x(t) \geq 1 - \varepsilon - b\varepsilon$. Since ε is arbitrary, one has $\liminf_{t\to\infty} x(t) \geq 1$. Therefore, $\lim_{t\to\infty} = 1$. □

To verify the stability switches, we numerically solve the system with some values of the parameters. Specifically, we choose values of the parameters according to [5], that $b = 1$, $a = 0.2$, $n = 0.01$. We then plot the function $Z_m(\tau)$. The Figure (2) shows some interesting property. For

$0 \leq m \leq 4$, each graph has two zeros within the feasible range of the delay parameter τ.

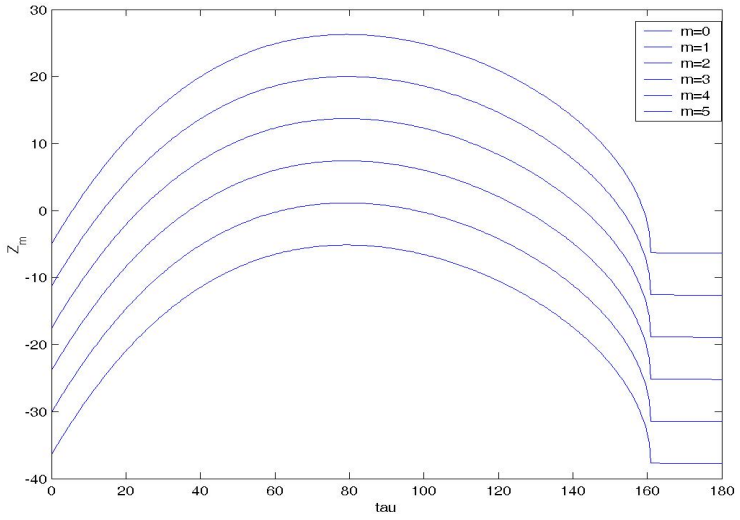

Figure 2: Plots of the functions $Z_m(\tau)$, $m = 0, 1, 2, 3, 4, 5$. Taking $b = 1$, $a = 0.2$, $n = 0.01$, the feasible range is $0 \leq \tau \leq \frac{1}{n} \ln \frac{b}{a} \approx 160$. From the top curve to the bottom curve, they are the graphs of $Z_0(\tau)$, $Z_1(\tau)$, ..., and $Z_5(\tau)$ respectively. It shows that for $0 \leq m \leq 4$, each $Z_m(\tau)$ has two intersection points with the horizontal line $\tau = 0$, and stability switch occur for each of $Z_m(\tau)$. When $m \geq 5$, $Z_m(\tau)$ has no intersection points with the horizontal line $\tau = 0$.

Unlike other stability switches causing by time delay where a solution of the system without delay is stable and it becomes unstable for some interval of the delay time and then it returns to stable status for even large delay times, the equilibrium solution $(1, 0)$ of the system (4) is unstable when the delay $\tau = 0$ under the condition $b > a$. As the delay time τ increases, it becomes stable within some delay time interval. Then, it becomes unstable again as the delay time increases. To demonstrate the stability switches, for chosen values of the parameters, $a = 0.2$, $b = 1$, $n = 0.01$ and $r = 1.5$,

each function $Z_m(\tau)$ for $m = 0, 1, 2, 3, 4$ has two zeros. The smaller root of $Z_0(\tau)$ is $\tau_{0,1} \approx 2.5$, and the smaller root of $Z_4(\tau)$ is $\tau_{4,1} \approx 62$. The equilibrium solution $(1, 0)$ is unstable when $0 \leq \tau \leq \tau_{0,1}$, and it is stable when $\tau_{0,1} \leq \tau \leq \tau_{4,1}$, it is unstable when $\tau > \tau_{4,1}$. However, when $\tau_{0,1} \leq \tau \leq \tau_{4,1}$, the corresponding periodic solutions are stable. The pictures in the left columns of the Figures (4)-(8) show these cases with various values of the delay parameter τ.

4.3 Stability of the interior equilibria $(x^*(\tau), y^*(\tau))$

At the interior equilibrium points $(x^*(\tau), y^*(\tau))$, where $x^*(\tau) = \frac{a}{b}e^{n\tau}$, $y^*(\tau) = \frac{1-\frac{a}{b}e^{n\tau}}{1+\frac{b}{r}}$, set $x = x^* + \bar{x}$, $y = y^* + \bar{y}$. Since each component of the interior equilibrium solutions is a function of the delay parameter τ, we write x^* as $x^*(\tau)$ when we would emphasize the delay parameter τ. The linearized system at (x^*, y^*) is given by:

$$X' = \begin{pmatrix} r - 2rx^* - ry^* & -rx^* \\ 0 & -a \end{pmatrix} \begin{pmatrix} \bar{x} \\ \bar{y} \end{pmatrix} + \begin{pmatrix} -by^*e^{-n\tau} & -bx^*e^{-n\tau} \\ by^*e^{-n\tau} & bx^*e^{-n\tau} \end{pmatrix} \begin{pmatrix} \bar{x}(t-\tau) \\ \bar{y}(t-\tau) \end{pmatrix}.$$

The characteristic equation is

$$\lambda^2 + (a - (r - 2rx^* - ry^*))\lambda + b(y^* - x^*)e^{-n\tau}e^{-\lambda\tau}\lambda$$
$$- a(r - 2rx^* - ry^*) + b(rx^* - 2rx_0^2 + ay^*)e^{-n\tau}e^{-\lambda\tau} = 0.$$

Substitute x^* and y^*, we have the characteristic equation,

$$\lambda^2 + a(\tau)\lambda + b(\tau)\lambda e^{-\lambda\tau} + c(\tau) + d(\tau)e^{-\lambda\tau} = 0, \tag{10}$$

where

$$a(\tau) = a - \frac{b - (2a + \frac{ar}{b})e^{n\tau}}{1 + \frac{b}{r}}, \quad b(\tau) = \frac{be^{-n\tau} - (2a + \frac{ab}{r})}{1 + \frac{b}{r}},$$

$$c(\tau) = \frac{-ab + a(2a + \frac{ar}{b})e^{n\tau}}{1 + \frac{b}{r}}, \quad d(\tau) = \frac{abe^{-n\tau} + (ab + ar - a^2) - \frac{2a^2r + 2a^2b}{b}e^{n\tau}}{1 + \frac{b}{r}}.$$

Assume the characteristic equation (10) has purely imaginary roots, $i\omega$, where $\omega > 0$. Then substituting it back to the equation, separating the real part and imaginary part, and using the identity $\sin^2\theta + \cos^2\theta = 1$, we get

$$\omega^4 - (b^2(\tau) + 2c(\tau) - a^2(\tau))\omega^2 + (c^2(\tau) - d^2(\tau)) = 0. \tag{11}$$

The roots of (11) are given by

$$\begin{aligned} \omega^+(\tau) &= \frac{1}{\sqrt{2}}\sqrt{b^2(\tau) + 2c(\tau) - a^2(\tau) + \Delta^{1/2}}, \\ \omega^-(\tau) &= \frac{1}{\sqrt{2}}\sqrt{b^2(\tau) + 2c(\tau) - a^2(\tau) - \Delta^{1/2}}, \end{aligned} \tag{12}$$

where

$$\Delta = (b^2(\tau) + 2c(\tau) - a^2(\tau))^2 - 4(c^2(\tau) - d^2(\tau)). \tag{13}$$

As in [2], we look for the values of the delay τ where the characteristic equation has purely imaginary roots, and they are given by zeros of the following functions

$$S_m^+ = \tau - \frac{\theta^+(\tau) + 2m\pi}{\omega^+(\tau)}, \quad S_m^- = \tau - \frac{\theta^-(\tau) + 2m\pi}{\omega^-(\tau)}, \tag{14}$$

where

$$\theta^\pm(\tau) = \arcsin\frac{(\omega^\pm(\tau)^2 - c(\tau))b(\tau) - a(\tau)d(\tau)}{\omega^\pm(\tau)^2 b^2(\tau) + d^2(\tau)}\omega^\pm(\tau).$$

We can compute the roots of the equation (11) by substituting coefficient functions $a(\tau)$, $b(\tau)$, $c(\tau)$ and $d(\tau)$. However, the symbolical computation will be extremely cumbersome. In stead, we will look at cases for given parameter values.

When $\tau = 0$, The characteristic equation (10) is reduced to

$$\lambda^2 + \frac{ar}{b}\lambda + \frac{ar(b-a)}{b} = 0. \tag{15}$$

When $b > a$, we have $\lambda_1(0)\lambda_2(0) = \frac{ar(b-a)}{b} > 0$ and $\lambda_1(0) + \lambda_2(0) = \frac{ar}{b} > 0$. Then, the real parts of two eigenvalues of the equation (15) are negative. Thus, the equilibrium point (x^*, y^*) is locally asymptotically stable, when $\tau = 0$.

Taking $b = 1, a = 0.2, n = 0.01$, these coefficients become,

$$a(\tau) = \frac{0.2 - 0.8r + r(0.4 + 0.2r)e^{\frac{\tau}{100}}}{1 + r}, \quad b(\tau) = \frac{re^{-\frac{\tau}{100}} - (0.2 + 0.4r)}{1 + r},$$

$$c(\tau) = \frac{-0.2r + 0.2r(0.4 + 0.2r)e^{\frac{\tau}{100}}}{1 + r}, \quad d(\tau) = \frac{0.2re^{-\frac{\tau}{100}} + r(0.08 + 0.12r)}{1 + r}.$$

When $r > 0.5$, $\Delta > 0$ for $\tau \geq 0$. If $r = 1.5$, $(\omega^+)^2 > 0$ for $0 \leq \tau \leq 79.2$, while $(\omega^-)^2 < 0$ for all feasible τ. Thus, we only consider S_m^+. In the feasible range, $S_0^+(\tau)$ has one zero, $\mu_{0,1} \approx 1.98$. $S_1^+(\tau)$ has two zeros, the bigger one is $\mu_{2,2} \approx 77$. Therefore, there exist stability switches start from this equilibrium solution $(\frac{a}{b}, \frac{1-\frac{a}{b}}{1+\frac{b}{r}})$. Figure (3) shows plots of functions S_m^+.

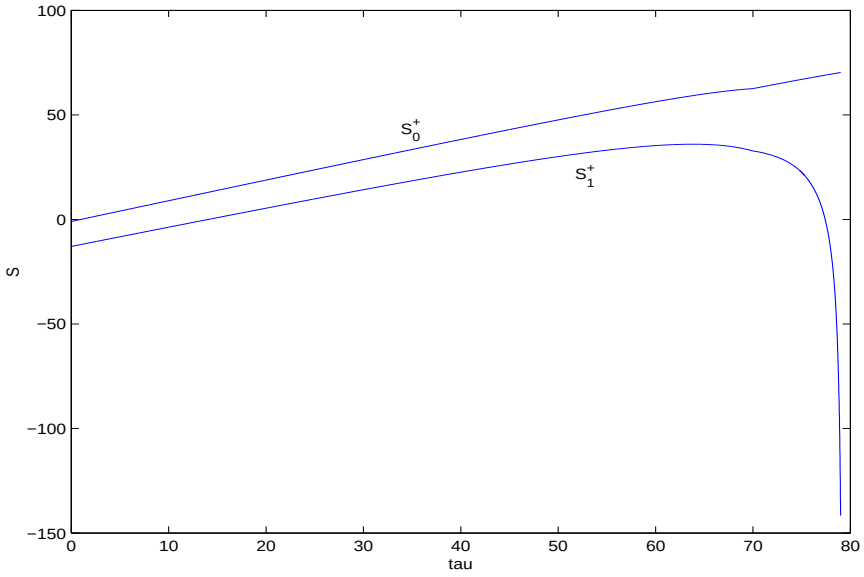

Figure 3: Plots of the functions $S_m^+(\tau)$, $m = 0, 1$. The parameter values are $b = 1$, $a = 0.2$, $n = 0.01$ and $r = 1.5$. Since the scale in the picture is relatively big, the intersection point of the function $S_0^+(\tau)$ and $\tau = 0$ is not clearly shown. However, the function $S_0^+(\tau)$ has a root, $\mu_{0,1} \approx 1.98$. The function $S_1^+(\tau)$ has two roots, $\mu_{2,1} \approx 14$ and $\mu_{2,2} \approx 77$.

The interior equilibrium is the function of the delay parameter τ, $(x^*(\tau), y^*(\tau))$. The interior equilibrium solution is locally asymptotical stable when $0 \leq \tau <$

$\mu_{0,1}$. The interior equilibrium solution is unstable when $\mu_{0,1} < \tau < \mu_{2,2}$, and is unstable when $\tau > \mu_{2,2}$. The pictures in the right columns of the Figures (4)-(8) show these cases with various values of the delay parameter τ.

Comparing the stability of the equilibrium solutions $(1, 0)$ and $(x^*(\tau), y^*(\tau))$, we observe that in some intervals of the delay parameter τ one equilibrium is stable while the other is unstable as shown in Figures (4)-(8). We obtain a rough picture of the dynamics of the model (4) as follows. The equilibrium $(0, 0)$ is always unstable. Without the delay, the equilibrium $(1, 0)$ is unstable while the equilibrium $(\frac{a}{b}, \frac{1-\frac{a}{b}}{1+\frac{b}{r}})$ is locally asymptotical stable. When the delay parameter τ is small, the interior equilibrium $(x^*(\tau), y^*(\tau))$ is still locally asymptotical stable and $(1, 0)$ is unstable. When the delay parameter τ is becoming greater, the equilibrium $(x^*(\tau), y^*(\tau))$ is unstable. When τ is even bigger, the equilibrium $(x^*(\tau), y^*(\tau))$ is stable again.

5 Discussion

The parameter b represents the non-dimensionalized infectivity of the virus while a represents the death rate of infected tumor cells. The theorem (4.2) states how these two parameters effect the virotherapy. When $b < a$, the equilibrium solution $x = 1$ and $y = 0$ is globally stable for any time delay. The tumor reaches its maximum size, and the therapy fails. On the other hand, from the viewpoint of epidemiology modeling, the condition $b < a$ implies the basic reproduction number

$$R_0 = \frac{\beta}{a} e^{-n\tau} = \frac{b}{aK} e^{-n\tau} = \frac{b}{a} \frac{1}{K} e^{-n\tau} < 1,$$

since the maximum size of the tumor is obviously greater than 1 and $e^{-n\tau} \leq 1$. Therefore, the infection can not spread out, and the infection free equilibrium is stable.

The relative sizes of the parameter a and b are dominant factors in virotherapy. In animal experiments, the viruses have high possibility to kill the tumor if the virus is more infectious. The virus has a high infectivity if it is more infectious to tumor cells. There are various genetic methods

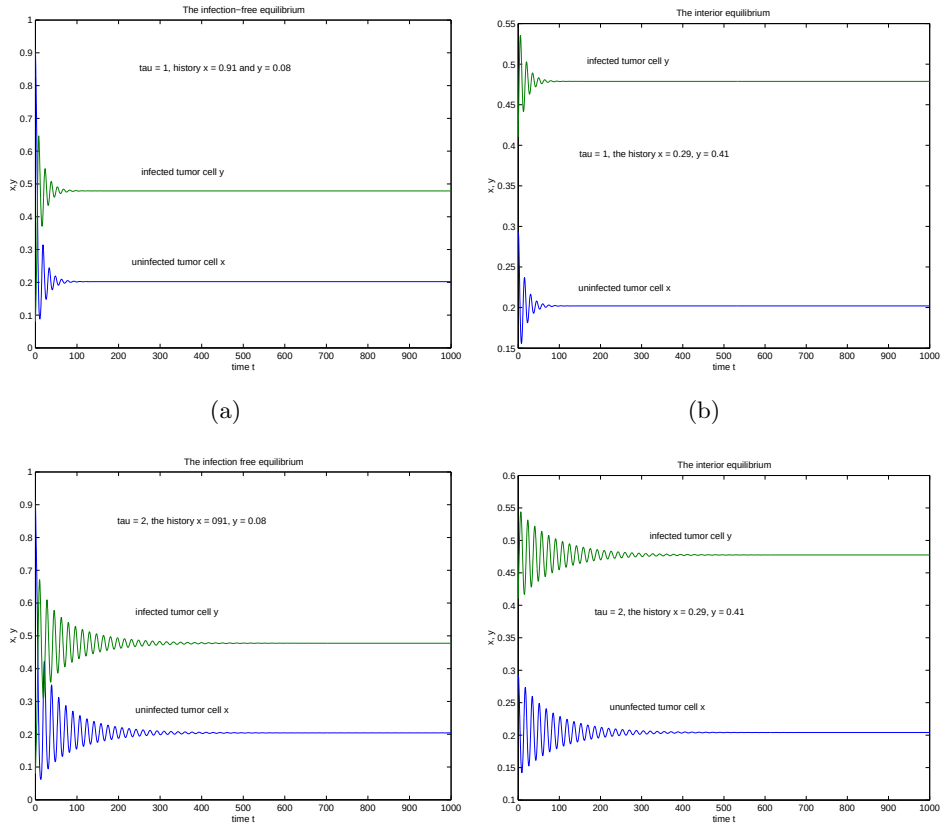

(a) (b)

(c) (d)

Figure 4: The pictures (a) and (c) show the equilibrium (1,0) is unstable, and the solutions start closely to (1,0) will diverge away to some interior equilibria, where $\tau = 1$ and $\tau = 2$ respectively and the history $x(\theta) = 0.91$ and $y(\theta) = 0.08$. The pictures (b) and (d) show the interior equilibria are locally asymptotical stable. Since the interior equilibria is the function of τ, the interior equilibria are corresponding to the delay parameter τ.

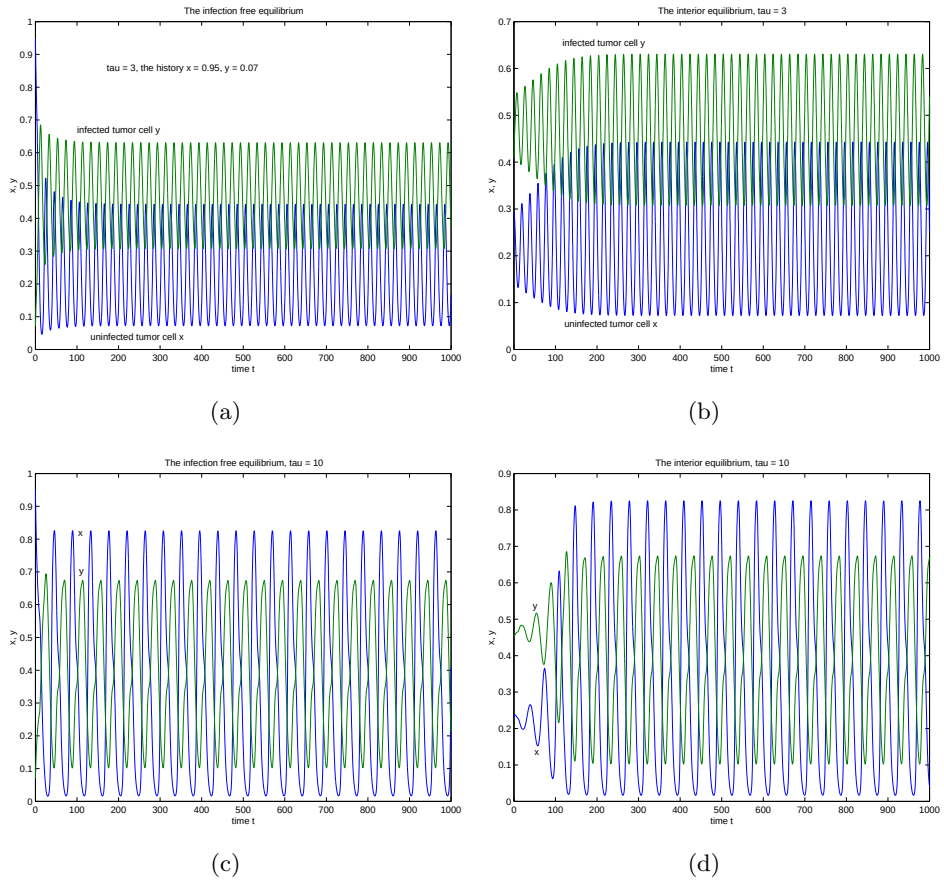

Figure 5: The pictures (a) and (c) show some solutions which start closely to (1,0), and they are periodic solutions, where $\tau = 3$ and $\tau = 10$ respectively, and the history $x(\theta) = 0.95$ and $y(\theta) = 0.07$. The pictures (b) and (d) show some solutions with the history $x(\theta) = 0.29$ and $y(\theta) = 0.41$, and $\tau = 3$ and $\tau = 10$ respectively.

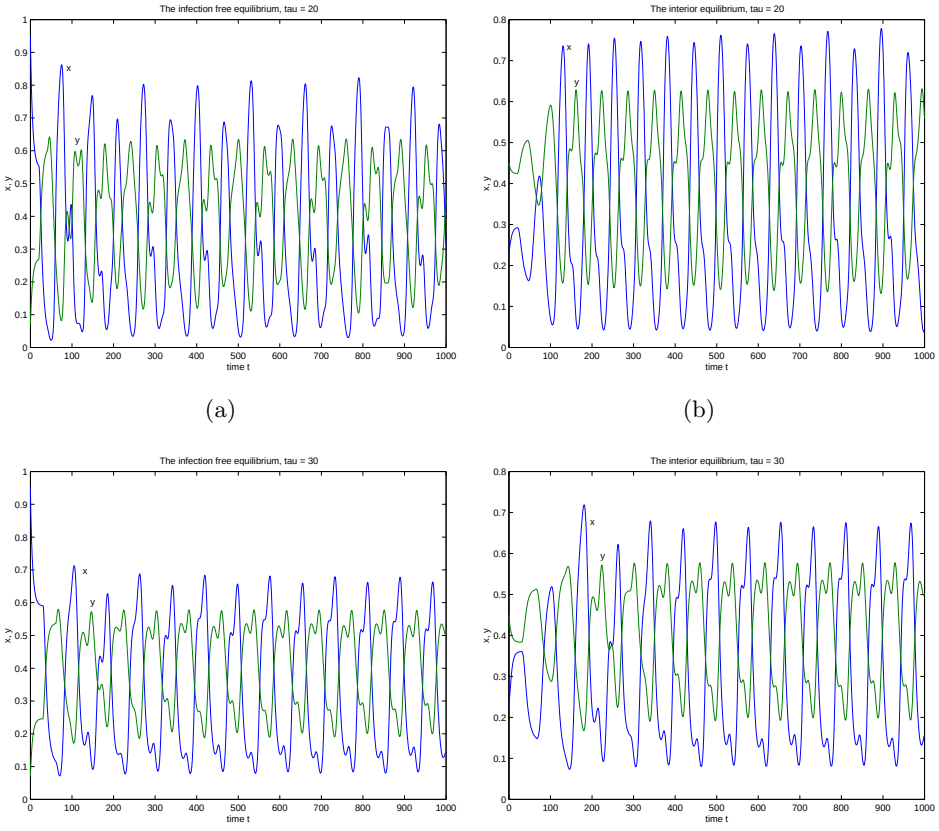

(a) (b)

(c) (d)

Figure 6: The pictures (a) and (c) show some solutions which start closely to (1,0), and they are periodic solutions, where $\tau = 20$ and $\tau = 30$ respectively, and the history $x(\theta) = 0.95$ and $y(\theta) = 0.07$. The pictures (b) and (d) show some solutions with the history $x(\theta) = 0.28$ and $y(\theta) = 0.45$, and $\tau = 20$ and $\tau = 30$ respectively.

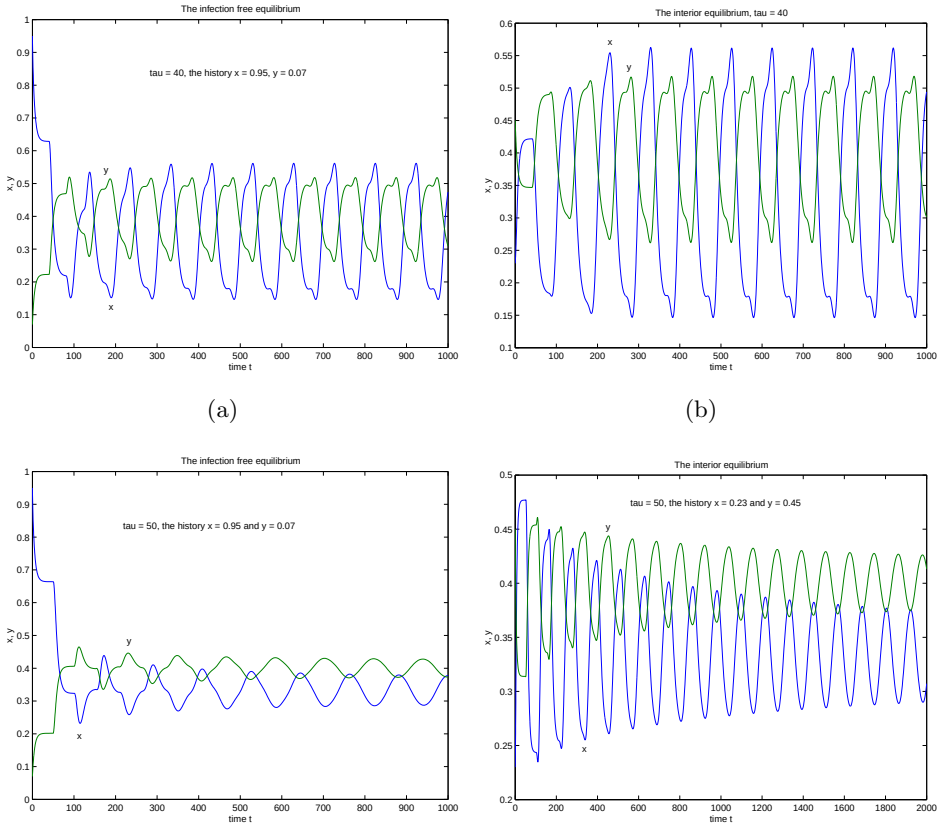

Figure 7: The pictures (a) and (c) show some solutions which start closely to (1,0), and they are periodic solutions, where $\tau = 40$ and $\tau = 50$ respectively, and the history $x(\theta) = 0.95$ and $y(\theta) = 0.07$. The pictures (b) and (d) show some solutions with the history $x(\theta) = 0.30$ and $y(\theta) = 0.45$, and $\tau = 40$ and $\tau = 50$ respectively.

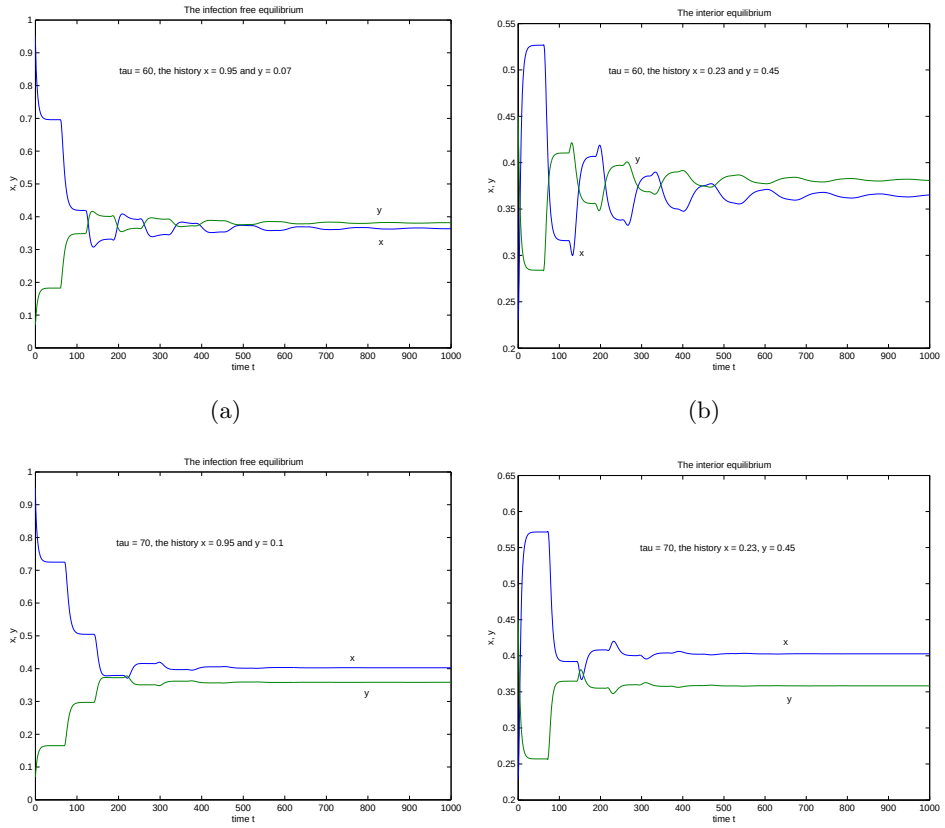

(a) (b)

(c) (d)

Figure 8: The pictures (a) and (c) show some solutions which start closely to (1,0), and they diverge but converge to some interior equilibrium solutions, where $\tau = 60$ and $\tau = 70$ respectively, and the history $x(\theta) = 0.95$ and $y(\theta) = 0.07$. The pictures (b) and (d) show some solutions with the history $x(\theta) = 0.30$ and $y(\theta) = 0.45$, and $\tau = 60$ and $\tau = 70$ respectively. These solutions converge to the corresponding interior equilibrium solutions.

that can be applied to modify the genomes of viruses so that the viruses have high infectivity [3]. Therefore, the virus with a low infectivity b that is smaller than the death rate of infected tumor cells can not be used to eradicate the tumor. However, when the infectivity is greater than the death rate of infected tumor cells $b > a$, the dynamics of virotherapy is much more complicated, where the intracellular viral life-cycle comes to play an important role.

Theoretically, when the infectivity b is greater than the death rate a of infected tumor cells, the viruses can not eradicate the tumor if the period of the intracellular viral life-cycle is ignored. As the equation (15) shown, it has two eigenvalues with negative real parts. The interior equilibrium solution (x^*, y^*) is locally asymptotical stable. In the feasible domain Σ of the model, there is a large port of the domain which is in the attractive range of this equilibrium point. That means, the tumor cells and infected tumor cells coexist, and the viruses can not eradicate the tumor. We also can see this point from the expression of the basic reproduction number $R_0 = \frac{\beta}{a} e^{-n\tau} = \frac{b}{aK} e^{-n\tau} = \frac{b}{a} \frac{1}{K}$. The condition $b > a$ alone can not guarantee $R_0 > 1$. Even b is big enough such that $R_0 > 1$, it only makes the interior equilibrium solution is locally asymptotical stable.

When the period of the intracellular viral life-cycle is incorporated into the model, but with the period modeled as the delay parameter, the tumor cells still can not be completely eradicated. When the delay parameter has a small value, tumor cells and infected tumor cells coexist, and the coexisting equilibrium solution is still locally asymptotical stable. If the viruses have a longer period of the intracellular viral life-cycle, the stability of the coexisting equilibrium solution will be broken. This creates a possibility of killing the tumor. Since the interior equilibrium solution is unstable in this case, the tumor cell population and the infected tumor cell population will not rest on a fixed level. Instead, they will periodically change over time or diverge away. The virotherapy seeks to decrease the tumor cell amount even it can not eradicate the tumor. The success of the therapy is determined by detectability of the tumor cells. Thus, it is considered as a successful

therapy if the tumor cell amount is below a detective level. In our case, it is possible that other parameters like the survival probability function can be chosen so that the periodic solution with lower tumor component. We then can obtain a good result of the virotherapy.

In many clinical and theoretical studies of virotherapy, the periodic phenomena were observed. When the value of the delay parameter is in this middle range, our model has stable periodic solutions. Thus, the intracellular viral life-cycle can explain periodic phenomena observed in [5, 14, 16] and other work.

However, when the intracellular viral life-cycle is too long, the interior equilibrium solution becomes locally asymptotical stable again. In this situation, the tumor cell component has even big quantity as $\frac{a}{b}e^{n\tau}$ is increasing function of τ. This is undesirable. When the intracellular viral life-cycle is even longer, the virotherapy totally fails since the interior equilibrium solution will be lost and there are only two equilibria $(0,0)$ and $(1,0)$.

Overall, a clinic implication is that the period of the intracellular viral life-cycle should also be modified when a type of a virus is modified for virotherapy, so that the period of the intracellular viral life-cycle is in a suitable range which can break the stability of the interior equilibrium solution.

Acknowledgment

The authors would like to thank the reviewer for helpful suggestions that lead to better model presentation. J.P. Tian gratefully acknowledges the support of a start-up fund at the College of William and Mary. Y. Kuang gratefully acknowledges support from National Science Foundation grants DMS-0436341 and DMS-0920744. H. Yang gratefully acknowledges support in part by the National Science Foundation of China under grant 10961025.

References

[1] Z. Bajzer, T. Carr, K. Josic, S.J. Russel, D. Dingli, *Modeling of cancer virotherapy with recombinant measles viruses*, J. Theoretical Biology, 252(2008), 109-122.

[2] E. Beretta, Y. Kuang, *Geometric stability switch criteria in delay differential systems with delay dependent parameters*, SIAM J. Anal. Vol. 33 (2002), No. 5, pp. 1144-1165.

[3] E.A. Chiocca, *Oncolytic viruses*, Nature reviews, Cancer. Vol. 2(2002), no. 12: 938-50.

[4] B.R. Dix, S.J. OCarroll, C.J. Myers, S.J. Edwards, A.W. Baithwaite, *Efficient induction of cell death by adenoviruses requires binding of E1B and p53*, Cancer Res. 60(2000), 26662672.

[5] A. Friedman, J.P. Tian, G. Fulci, E.A. Chiocca, J. Wang, *Glioma virotherapy: effects of innate immune suppression and increased viral replication capacity*, Cancer Research, Vol.66 (2006), 2314-2319.

[6] A.R. Hall, B.R. Dix, S.J. OCarroll, A.W. Braithwaite, *p53-dependent cell death/apoptosis is required for a productive adenovirus infection*, Nature Med. 4(1998), 10681072.

[7] J.N. Harada, A.J. Berk, *p53-independent and -dependent requirements for E1B-55k in adenovirus type 5 replication*, J. Virol. 73(1999), 53335344

[8] E. Kelly and S.J. Russell, *History of Oncolytic Viruses: Genesis to Genetic Engineering, Molecular Therapy*, Molecular Therapy, 15(2007), no. 4, 651659.

[9] K.A. Parato, D. Senger, A.J. Forsyth and J.C. Bell, *Recent progress in the battle between oncolytic viruses and tumours, Nature reviews*, Cancer, Vol. 5(2005), 965-976.

[10] H. Kambara, H. Okano, E.A. Chiocca, Y. Saeki, *An oncolytic HSV-1 mutant expressing ICP34.5 under control of a nestin promoter increases survival of animals even when symptomatic from a brain tumor*, Cancer Res. 65(2005), no. 7, 2832-2839.

[11] N.L. Komarova, D. Wodarz, *ODE models for oncolytic virus dynamics*, J Theor Biol. 263(2010), no. 4, 530-43.

[12] T.-C. Liu and D. Kirn, *Systemic efficacy with oncolytic virus therapeutics: clinical proof-of-concept and future directions*, Cancer Res. 67(2007): 429-432.

[13] M. Ramachandra, et al. *Re-engineering adenovirus regulatory pathways to enhance oncolytic specificity and efficacy*, Nature Biotechnol. 19(2001), 10351041.

[14] J.P. Tian, *The replicability of oncolytic virus: defining conditions in tumor virotherapy*, Math. Biosci. Eng. 8(2011), 841-860.

[15] Y. Tao, Q. Quo, *The competitive dynamics between tumor cells, a replication-competent virus and an immune response*, J. Math. Biol. 51(1) (2005), 37-78.

[16] J.T. Wu, H.M. Byrne, D.H. Kirn, L.M. Wein, *Modeling and analysis of a virus that replicates selectively in tumor cells*, Bull. Math. Biol. 63 (2001) (4), 731-768.

[17] L.M. Wein, J.T. Wu, D.H. Kirn, *Validation and analysis of a mathematical model of a replication-competent oncolytic virus for cancer treatment: implications for virus design and delivery*, Cancer Res. 63(6)(2003), 1317-1324.

[18] D. Wodarz, *Viruses as antitumor weapons: defining conditions for tumor remission*, Cancer Res. 61(2001), 3501-3507.

[19] D. Wodarz, N.L. Komarova, *Towards predictive computational models of oncolytic virus therapy: basis for experimental validation and model selection*, PloS ONE, Vol.4 (2009), (1), e4271.

[20] A.S. Novozhilov, F.S. Berezovskaya, E.V. Koonin, G.P. Karev, *Mathematical modeling of tumor therapy with oncolytic viruses: Regimes with complete tumor elimination within the framework of deterministic models*, Biology Direct, 1:6 (2006), 1-18.